



# Nitrous oxide (N<sub>2</sub>O) in the sea surface microlayer and underlying water during a phytoplankton bloom: a mesocosm study

Ina Stoltenberg<sup>1</sup>, Lea Lange<sup>1</sup>, and Hermann W. Bange<sup>1</sup>

5 <sup>1</sup>Marine Biogeochemistry, GEOMAR Helmholtz Centre for Ocean Research Kiel, Kiel, 24148, Germany

Correspondence to: Ina Stoltenberg ([istoltenberg@geomar.de](mailto:istoltenberg@geomar.de)), Hermann Bange ([hbange@geomar.de](mailto:hbange@geomar.de))

**Abstract.** Nitrous oxide (N<sub>2</sub>O) is an important climate-relevant atmospheric trace gas. The open and coastal oceans are a major source for atmospheric N<sub>2</sub>O. However, its production and consumption pathways in the ocean are not well-known and its emissions estimates are associated with a high degree of uncertainty. Potential N<sub>2</sub>O production pathways in the oxic surface ocean include microbial nitrification, release from phytoplankton and photochemodenitrification. In order to decipher the effect of a phytoplankton bloom on dissolved N<sub>2</sub>O concentrations, N<sub>2</sub>O was measured – for the first time – in the sea surface microlayer (SML, i.e. the upper 1 mm of the water column) and in the corresponding underlying water (ULW) during a mesocosm study with Jade Bay (southern North Sea) water from 16 May to 16 June 2023. N<sub>2</sub>O concentrations were slightly enriched in the SML compared to the ULW although the difference of the mean N<sub>2</sub>O concentrations between the ULW and SML was statistically not significant. However, the enrichment of N<sub>2</sub>O in the SML was most probably underestimated due to the loss of N<sub>2</sub>O during sampling with the glass plate method. N<sub>2</sub>O was supersaturated (100% – 157%) in the ULW and SML during the course of the study which indicated an in-situ production of N<sub>2</sub>O. N<sub>2</sub>O in-situ production was most probably driven by photochemodenitrification in combination with the release from phytoplankton whereas microbial production of N<sub>2</sub>O via nitrification appeared to be of minor importance. N<sub>2</sub>O concentrations in both the ULW and the SML were remarkably constant over time and were apparently not affected by irradiation and a phytoplankton bloom which was triggered by nutrient additions. We therefore conclude that the N<sub>2</sub>O in-situ sources were balanced by the release of N<sub>2</sub>O to the atmosphere resulting in a steady state of the system. Our results indicate that the role of the SML for N<sub>2</sub>O cycling in the surface ocean and its emissions to the atmosphere has been overlooked so far. Moreover, our results are in line with results from field studies which showed that phytoplankton blooms in the ocean do not result in temporarily enhanced N<sub>2</sub>O concentrations in the ocean surface layer.

## 1 Introduction

Nitrous oxide (N<sub>2</sub>O) is a climate-relevant, long-lived trace gas in the Earth's atmosphere: In the troposphere it acts as a strong greenhouse gas and in the stratosphere it is one of the major ozone-depleting compounds (IPCC, 2021). The open and coastal oceans contribute about 25 % to the natural and anthropogenic emissions of atmospheric N<sub>2</sub>O (Tian et al., 2024). Natural N<sub>2</sub>O production is part of the nitrogen cycle where it occurs as a by-product during nitrification (i.e. microbial oxidation of ammonia to nitrite and nitrate) and as an intermediate during denitrification (i.e. microbial reduction of nitrate via N<sub>2</sub>O to dinitrogen) (see e.g. Bange et al., 2024) Only recently it was shown that in aquatic environments N<sub>2</sub>O is also produced photochemically via photochemodenitrification from dissolved nitrite (Leon-Palmero et al., 2025). Moreover, N<sub>2</sub>O is also released from cultures of marine phytoplankton (McLeod et al., 2021; Plouviez et al., 2019; Teuma et al., 2023). However, phytoplankton blooms in the ocean



which were triggered by artificial or natural iron fertilization showed that phytoplankton blooms not necessarily lead to enhanced  $N_2O$  production (Fariás et al., 2015; Law and Ling, 2001; Walter et al., 2005).  $N_2O$  cycling in the ocean is, thus, usually described as being dominated by microbial production and consumption pathways such as nitrification and denitrification. The contributions by its photochemical production and release by phytoplankton are unknown or associated with large uncertainties, respectively.

The sea surface microlayer (SML) forms the interface between the ocean and the atmosphere. It is ubiquitous in the open and coastal oceans and thus covers about 71% of the Earth's surface, with a thickness of up to 1 mm (Engel et al., 2017). The SML plays a key role for the exchange of momentum, heat, gases and aerosols between the ocean and the atmosphere. Despite its comparably small volume, it is a distinct water layer which differs from the underlying (i.e. subsurface) water (ULW) in its physical properties as well as its chemical and biological composition (Cunliffe et al., 2013; Engel et al., 2017; Wurl et al., 2017; 2021). Dissolved nutrients (e.g. nitrite) as well as surface-active organic compounds (surfactants) which originate from biological production can accumulate in the SML (Wurl et al., 2011; Zhou et al., 2018). There are direct and indirect hints that especially the accumulation of surfactants in the SML affects the exchange of  $N_2O$  across the water/atmosphere interface (Kock et al., 2012; Mesarchaki et al., 2015). Moreover, processes in the SML seem to result in different transfer velocities for the release of  $N_2O$  from the water side (evasion) and uptake of  $N_2O$  from the air side (invasion) (Conrad and Seiler, 1988; Upstill-Goddard et al., 2003).

However, the determination of trace gases in the SML is difficult because of the limited access to the SML in combination with the inherent problems of gas loss with the usually applied SML sampling methods (i.e. the glass plate and related methods). To the best of our knowledge,  $N_2O$  concentrations have not been determined in the SML so far.

Here we present the first time-series measurement of  $N_2O$  concentrations in both the SML and the ULW during a mesocosm study in May/June 2023 (Bibi et al., 2025). The overarching objectives of our study were (1) to assess whether there is an accumulation of  $N_2O$  in the SML and (2) to decipher the effect of enhanced biological production on dissolved  $N_2O$  in the water column.

## 2 Methods

The mesocosm study was part of the BASS (Biogeochemical processes and Air–sea exchange in the Sea-Surface microlayer) project and took place in one of the mesocosms at the Sea Surface Facility (SURF) of the University of Oldenburg in Wilhelmshaven, Germany, between 16 May to 16 June 2023.

### 1.1 Mesocosm setup

A detailed description of the mesocosm facility and the BASS study is given in Bibi et al. (2025). The mesocosm basin was filled with water from the adjacent Jade Bay which is a shallow bay with water depths  $<20$  m on the southern North Sea coast. The mesocosm basin was filled with particle-reduced Jade Bay water on 13 May 2023. Subsequently, fleece filtration and protein skimming were initiated under slow water circulation for three consecutive days. Small pumps were used (1) to ensure the homogeneity of the water column and reduce stratification and (2) to reduce particle settling and biofilm formation on walls and bottom of the basin. For details of the pre-treatment of the Jade Bay water and the setup of the pump array see Bibi et al. (2025). On 15 May 2023, the surface layer of the water column was skimmed with glass plates for nine hours to remove any visible organic



75 film residues and debris from the water surface. Regular sampling for dissolved  $N_2O$  from the SML and the ULW started on 16 May. Jade Bay water was replenished with 4.5 L per day to replace the water removed by the sampling of the SML and the ULW in order to maintain a constant water volume in the basin.

Measurements during the study included various physical, biological and chemical parameters. Here we show the water temperature, salinity, nitrate/nitrite and chlorophyll concentrations which correspond to our  $N_2O$  concentration measurements. For details of the applied methods and instruments see the overview in Bibi et al. (2025).

In order to trigger a phytoplankton bloom, nutrients (nitrate, phosphate and silicate) were added on 26 May, 30 May and 1 June 2023 (for details of the nutrient addition, such as the added concentrations, see Bibi et al., 2025). The mesocosm facility has a retractable roof of transparent polycarbonate plates. The roof was open during the day and the basin was exposed to day light whereas the roof was closed during the night and rain events. The length of the days increased from 16 hours on 16 May to 17 hours on 16 June 2023 (see <https://www.sunrise-and-sunset.com/de/sun/deutschland/wilhelmshaven/2023/mai>; last access on 15 September 2025).

### 1.2 $N_2O$ sampling

All samples for  $N_2O$  were collected in triplicates in 20 mL amber glass vials, bubble-free and crimped air-tight with butyl rubber stoppers and aluminium caps. SML samples for  $N_2O$  were taken every three days alternating either 30 minutes past sunrise or 10 hours past sunrise. The SML samples were taken with a glass plate (Cunliffe and Wurl, 2014). The water from the glass plate was transferred to the glass vials using a wiper and a funnel. Samples from the ULW were collected twice a day (30 minutes past sunrise and 10 hours past sunrise) on days with no SML sampling for  $N_2O$  and three times a day on days with SML sampling for  $N_2O$  including one night (dark) sample taken about two hours after sunset. Diurnal (24h) cycles were sampled from the UWL on 24 May, 2 June, 4 June and 8 June 2023 with a time interval of two hours. Samples from the ULW were taken by using a Teflon<sup>®</sup> hose which was placed into the mesocosm using a lab stand to maintain a sampling depth of 0.6 m.

To stop any microbial or other biological processes which might influence  $N_2O$  production or consumption in the sample, all samples were poisoned as quick as possible (usually within one hour) after sampling by adding 0.05 mL of oversaturated aqueous solution of mercury(II) chloride ( $HgCl_2$ ). Samples were inverted after poisoning to ensure that the added  $HgCl_2$  solution was distributed evenly throughout the sample. Samples were stored at room temperature and in the dark until measurement in our laboratory at GEOMAR in Kiel. All samples were measured within 21 months after the study. A comparably long storage time, however, should not affect the  $N_2O$  concentrations as (Wilson et al., 2018) pointed out.

### 1.3 $N_2O$ concentration measurements

$N_2O$  concentrations were determined with the static headspace technique in combination with a gas chromatograph (Hewlett-Packard 5890A Series II) equipped with an electron capture detector for separation of  $N_2O$  from the gas mixture and detection, respectively. We replaced 10 mL of the seawater sample by injecting helium with a gas tight syringe. After agitation on a Vortex mixer, samples were left to equilibrate for two hours. Subsequently, a subsample of 9 mL was taken from the headspace with a gas tight syringe and injected manually into the gas chromatograph. Before flushing the 2 mL sample loop the sample was dried by passing through a moisture trap filled with phosphorous pentoxide (Sicapent<sup>®</sup>, Merck Germany). A mixture of Argon (5 %) and Methane was used as a carrier gas and gas chromatographic separation was executed at 190 °C on a packed molecular sieve column



(6ft × 1/8" SS, 5Å, mesh 80/100, Alltech GmbH, Germany). For calibration, two standard gas mixtures (working standards) of N<sub>2</sub>O in synthetic air with dry mole fractions of 391.46 ± 9.80 ppb and 1055.99 ± 7.91 ppb N<sub>2</sub>O were used (Deuste Gas Solution GmbH, Schömburg, Germany). The working standards have been calibrated against a primary N<sub>2</sub>O standard gas mixture provided by the National Oceanic and Atmospheric Administration (NOAA PMEL, Seattle, Wa, USA; for details see Wilson et al., 2018). The concentrations of dissolved N<sub>2</sub>O (C<sub>N2O</sub>) in the SML and ULW samples were computed with Eq. (1):

$$C_{N2O} = \beta * x' * P + (x' * P / RT) * (V_{hs} / V_{wp}) \quad (1)$$

where  $\beta$  is the Bunsen solubility (in nmol L<sup>-1</sup> atm<sup>-1</sup>) of N<sub>2</sub>O calculated as a function of salinity and temperature at the time of equilibration (Weiss and Price, 1980). T is the temperature at the time of equilibration. P is the atmospheric pressure (set to 1 atm). V stands for the volume of the water phase (wp) and the headspace (hs) in mL. R is the gas constant (8.2057 10<sup>-5</sup> m<sup>3</sup> atm K<sup>-1</sup> mol<sup>-1</sup>) and x' is the dry mole fraction of N<sub>2</sub>O in ppb (= 10<sup>-9</sup>). The average relative measurement error of the average N<sub>2</sub>O concentrations (= mean of the triplicates) was ± 4.5%.

#### 1.4 N<sub>2</sub>O enrichment factors and saturations

N<sub>2</sub>O enrichment factors (EF<sub>N2O</sub>) are given as (C<sub>N2O</sub>)<sub>SML</sub> / (C<sub>N2O</sub>)<sub>ULW</sub> and N<sub>2</sub>O saturations (Sat<sub>N2O</sub> in %) were computed according to Eq. (2):

$$Sat_{N2O} = 100 * C_{N2O} / C_{eq} \quad (2)$$

where C<sub>eq</sub> is the equilibrium concentration of N<sub>2</sub>O calculated with the solubility Eq. of (Weiss and Price, 1980) by using the water temperature and salinity at the time of sampling and the average monthly atmospheric dry mole fraction of 337.6 ppb N<sub>2</sub>O for May/June 2023 measured at the AGAGE (Advanced Global Atmospheric Gases Experiment) monitoring station in Mace Head at the west coast of Ireland ((Prinn et al., 2018); dataset doi:10.3334/CDIAC/ATG.DB1001 accessed via <https://data.ess-dive.lbl.gov/datasets/doi:10.3334/CDIAC/ATG.DB1001> on 15 September 2025).

#### 1.5 Photochemical N<sub>2</sub>O production

N<sub>2</sub>O production rates via photochemodenitrification (PR<sub>ped</sub> in nmol N<sub>2</sub>O L<sup>-1</sup> h<sup>-1</sup>) were estimated with Eq. (3) given in (Leon-Palmero et al., 2025):

$$PR_{ped} = 0.5/24 * 0.32 * \exp(0.23 * C_{NO2-}) \quad (3)$$

where C<sub>NO2-</sub> is the concentration of dissolved NO<sub>2</sub><sup>-</sup> in μmol L<sup>-1</sup> in the ULW or in the SML and the factor 0.5/24 is the conversion factor from nmol N L<sup>-1</sup> d<sup>-1</sup> to nmol N<sub>2</sub>O L<sup>-1</sup> h<sup>-1</sup>.

#### 1.6 N<sub>2</sub>O air-sea gas exchange

A rough estimate of the average N<sub>2</sub>O gas exchange (F<sub>asc</sub> in nmol N<sub>2</sub>O L<sup>-1</sup> h<sup>-1</sup>) was computed according to the approach of (Liss and Merlivat, 1986) (Eq. 4). The approach of Liss and Merlivat (1986) was chosen because it was derived mainly from wind/water tunnel studies which do have wind/wave features comparable to the



mesocosm study (e.g. in view of the wind fetch) and therefore seems to be more appropriate than the usually used approaches derived from open ocean studies which do have significantly different wind/wave features (see e.g. Wanninkhof, 2014).

155

$$F_{\text{asc}} = 0.17 * (0.01/d) * u_{10} * (C_{\text{N}_2\text{O}} - C_{\text{eq}}) * (600 * Sc^{-2/3}) \quad (4)$$

160

where  $u_{10}$  is the average wind speed in 10 m height ( $= 0.9 \pm 0.6 \text{ m s}^{-1}$ ),  $d$  is set to the average thickness of the SML during the study (0.001 m, see Rauch et al., 2025) or the overall water depth of the mesocosm basin (0.8 m),  $C_{\text{N}_2\text{O}}$  is the  $\text{N}_2\text{O}$  concentration in the SML or in the ULW, 0.01 is the conversion factor from cm to m and  $Sc$  is the Schmidt number which was computed using the empirical Eq.s for the kinematic viscosity of seawater (Siedler and Peters, 1986) and the diffusion coefficient of  $\text{N}_2\text{O}$  in water (Rhee, 2000). The overall water depth of the basin was applied with the assumption that the water column in the basin was well-mixed during the study.  $F_{\text{asc}}$  was set to 0 when the roof of the mesocosm facility was closed.

165

## 2 Results

### 2.1. Overview of general conditions and parameters in the mesocosm

Chlorophyll a concentrations varied from 1.0 to 11.4  $\mu\text{g L}^{-1}$  and were affected by the nutrient additions which triggered a phytoplankton bloom (Bibi et al., 2025). Three phases of the bloom have been identified: 1) a pre-bloom phase from the start of the study until 26 May 2023, 2) a bloom phase from 27 May until 4 June 2023 and 3) the post-bloom phase from 5 June 2023 until the end of the study (Bibi et al., 2025). Haptophytes, specifically *Emiliania huxleyi* (*Gephyrocapsa huxleyi*), dominated the phytoplankton community, followed by diatoms, primarily *Cylindrotheca closterium* (Bibi et al., 2025). Enrichments of surfactants and dissolved organic carbon were observed after the bloom (data are shown in Bibi et al., 2025, Asmussen-Schäfer et al., 2025). Water temperatures were in the range of 16.6 and 20.3 °C until 2 June 2023 and then started to increase up to 24.3 °C on 12 June 2023. The salinity increased almost linearly during the study from 28.98 to 32.28 (Fig. 1).

175

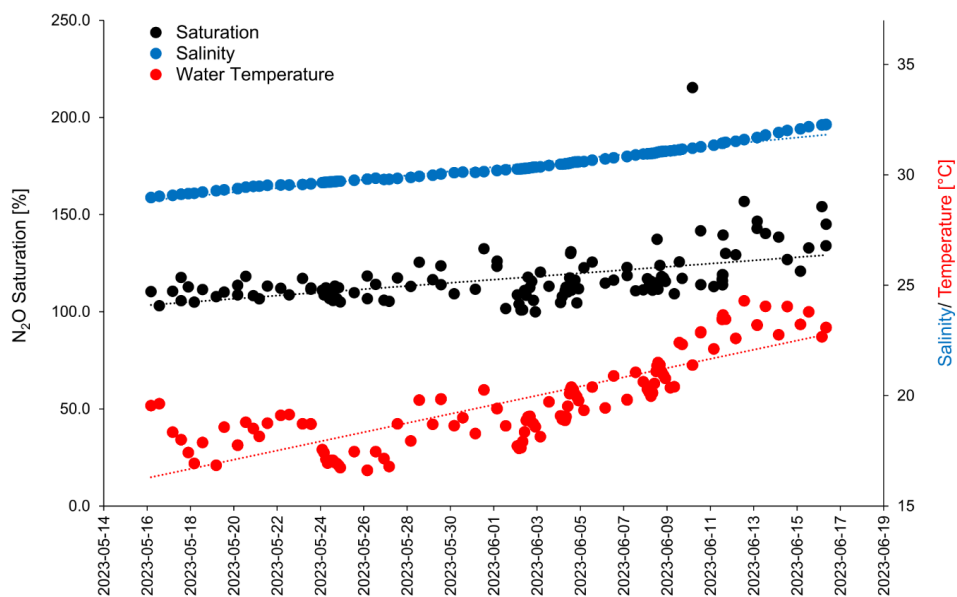


Figure 1: Water temperature, salinity and N<sub>2</sub>O saturation during the mesocosm study.

Nitrate (NO<sub>3</sub><sup>-</sup>) and nitrite (NO<sub>2</sub><sup>-</sup>) in the ULW and the SLM, as well as nutrient additions to the mesocosm are shown in Fig. 2 (Bibi et al., 2025).

180

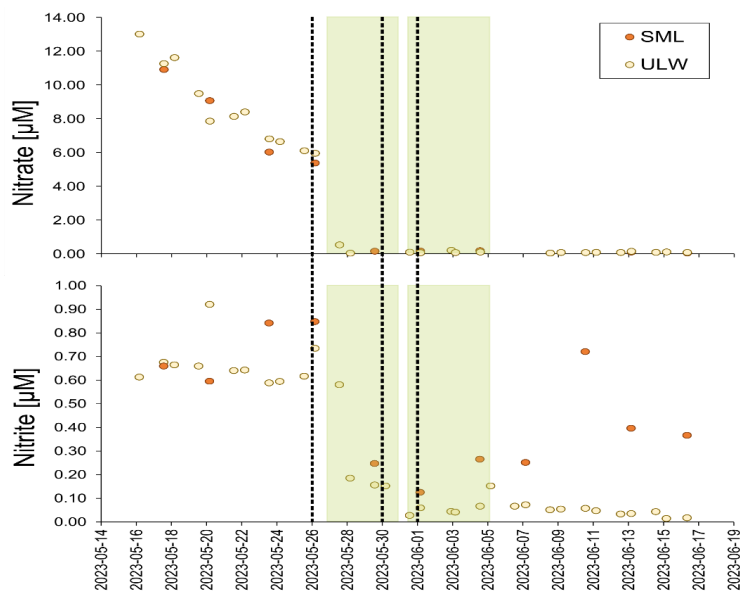


Figure 2: Dissolved nitrate (upper panel) and dissolved nitrite (lower panel) during the mesocosm study in the SML (filled red circles) and the ULW (open circles). µM stands for 10<sup>-6</sup> mol L<sup>-1</sup>. The bloom is indicated by the green-shaded boxes. The timing of the nutrient additions is indicated by the three dashed lines.

185

7

$\text{NO}_3^-$  concentrations decreased steadily from the start of the study until the onset of the bloom on 27 May 2023. This was followed by a sharp drop of  $\text{NO}_3^-$  concentrations which remained low ( $0.03 - 0.52 \mu\text{mol L}^{-1}$ ) until the end of the study. Nitrite concentrations in both the ULW and SML dropped down as well when the bloom started on 27 May 2023. During the bloom and post-bloom phases the  $\text{NO}_2^-$  concentrations remained low, whereas, the  $\text{NO}_2^-$  concentrations in the SML increased again in the post-bloom phase to a maximum concentration of  $>1 \mu\text{mol L}^{-1}$  until 14 June 2023 (Bibi et al., 2025). With the exception of 20 May 2023,  $\text{NO}_2^-$  was always enriched in the SML.

## 2.2. $\text{N}_2\text{O}$ concentrations, saturation and enrichment

$\text{N}_2\text{O}$  concentrations in the SML and the ULW as well as chlorophyll a concentrations are shown in Fig. 3.

195

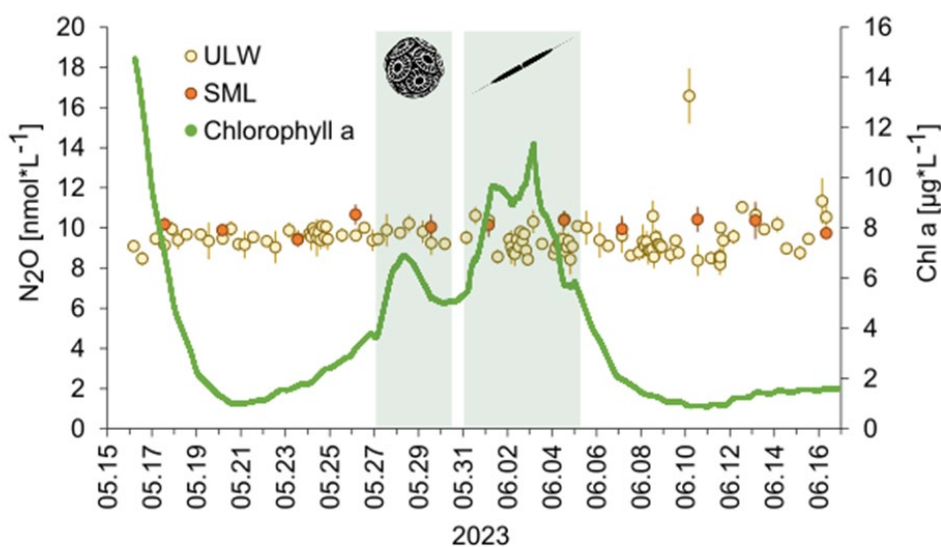


**Figure 3:**  $\text{N}_2\text{O}$  concentrations in the SML (filled red circles) and ULW (open circles) and chlorophyll a during the mesocosm study (green line). The green shaded boxes indicate the bloom. The inserted pictures show the haptophyte *Emiliania huxleyi* (*Gephyrocapsa huxleyi*) (left) and the diatom *Cylindrotheca closterium* (right).

$\text{N}_2\text{O}$  concentrations ranged from  $9.4$  to  $10.7 \text{ nmol L}^{-1}$  and from  $8.2$  to  $16.6 \text{ nmol L}^{-1}$  in the ULW and the SML, respectively. There were no temporal trends for  $\text{N}_2\text{O}$  in the ULW and the SML. The overall average  $\text{N}_2\text{O}$  concentrations ( $\pm$  standard deviation) in the ULW was  $9.4 \pm 0.6 \text{ nmol L}^{-1}$  (excluding the single maximum concentration of  $16.6 \text{ nmol L}^{-1}$ ). The average  $\text{N}_2\text{O}$  concentrations for the samples taken in parallel for SML and UWL were  $10.1 \pm 0.4$  and  $9.7 \pm 0.7 \text{ nmol L}^{-1}$ , respectively. However, the difference between the average  $\text{N}_2\text{O}$  concentrations in the SML and the UWL was not significant according to the Student's t-test (two tailed, different variances,  $p > 0.05$ ). The average  $\text{N}_2\text{O}$  concentration during the day was  $9.4 \pm 0.7 \text{ nmol L}^{-1}$  and the average  $\text{N}_2\text{O}$  concentration during the night was  $9.5 \pm 0.6 \text{ nmol L}^{-1}$  (excluding the single maximum concentration of  $16.6 \text{ nmol L}^{-1}$ ). Diurnal cycles of  $\text{N}_2\text{O}$  concentrations in the ULW and light irradiance are shown in Fig. 4. There were no diurnal trends.

210

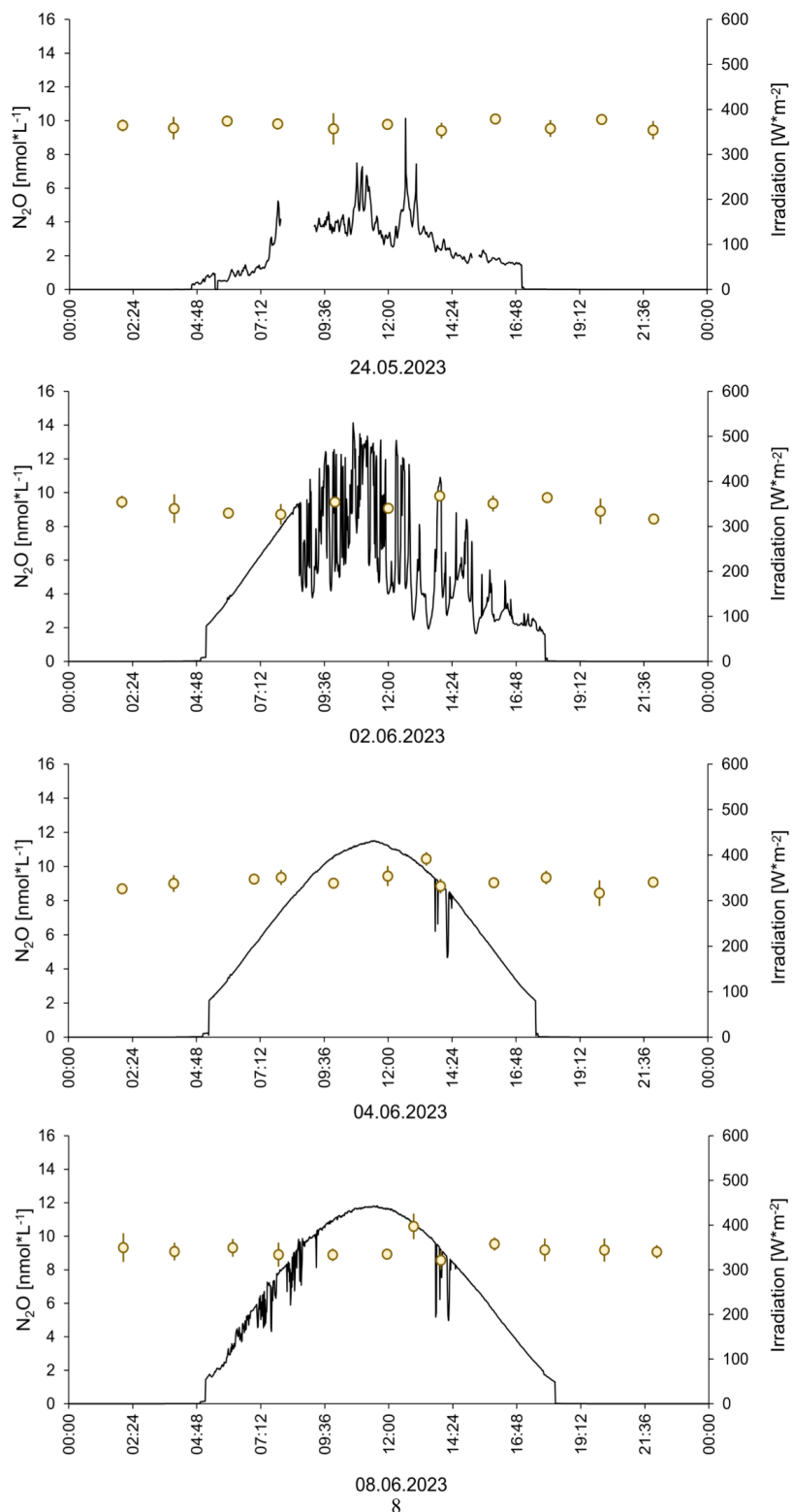






**Figure 4: 24h measurements of N<sub>2</sub>O concentrations on four days during the mesocosm study. The irradiance at a wavelength of 356 nm is shown.**

N<sub>2</sub>O saturations in the SML and the ULW were in the range from 100 to 157 % (215 % for the single maximum concentration from the ULW, Fig. 1). The enrichment factor of N<sub>2</sub>O in the SML was in the range from 0.9 to 1.2 and the average enrichment factor ( $\pm$  standard deviation) was  $1.1 \pm 0.1$  indicating an overall enrichment. However, in a few cases  $EF_{N_2O} < 1.0$  was observed as well.

### 2.3. N<sub>2</sub>O production and gas exchange

N<sub>2</sub>O production rates via photochemodenitrification ( $PR_{ped}$ ) were calculated only for daylight samples and ranged from 0.0071 to 0.0081 nmol N<sub>2</sub>O L<sup>-1</sup> h<sup>-1</sup> and from 0.0067 to 0.0078 nmol N<sub>2</sub>O L<sup>-1</sup> h<sup>-1</sup> in the SML and ULW, respectively (Table 1). Although the mean  $PR_{ped}$  in the SML ( $0.0075 \pm 0.0004$  nmol L<sup>-1</sup> h<sup>-1</sup>) was slightly higher compared to the  $PR_{ped}$  in the ULW ( $0.0071 \pm 0.0005$  nmol L<sup>-1</sup> h<sup>-1</sup>), there was no statistically significant difference between the mean  $PR_{ped}$  in the SML and the UWL. The N<sub>2</sub>O gas exchange ( $F_{ase}$ ) was in the range from 0 to 4.8 nmol N<sub>2</sub>O L<sup>-1</sup> h<sup>-1</sup> and 0 to 0.0081 nmol L<sup>-1</sup> h<sup>-1</sup> for the average thickness of the SML and the overall water depth (including N<sub>2</sub>O concentrations from the SML and UWL, respectively (Table 1).

Table 1: Potential N<sub>2</sub>O sources and sinks (in nmol L<sup>-1</sup> h<sup>-1</sup>). Sd stands for standard deviation.

	Average $\pm$ sd	Minimum	Maximum	Remarks	References
<b>Sources</b>					
Photochemodenitrification in the SML	0.0075 $\pm$ 0.0004	0.0071	0.0081	Estimated, occurs only during day time	This study
Photochemodenitrification in the UWL	0.0071 $\pm$ 0.0005	0.0067	0.0078	Estimated, occurs only during day time	This study
<i>E. hux</i> ( <i>G. hux</i> )	0.11 $\pm$ 0.02			culture	(McLeod et al., 2021)
Diatoms		-0.01	0.3	cultures	(McLeod et al., 2021, Teuma et al., 2023)
Nitrification		0.0001	0.0003	Measurements from a coastal site (Boknis Eck)	(Leon-Palmero et al., 2025)
<b>Sink</b>					
Gas exchange (SML)	1.7 $\pm$ 1.9	0	4.8	Estimated for the SML (0.001 m) only; gas exchange was set to 0 when the roof was closed	This study
Gas exchange (SML + ULW)	0.0014 $\pm$ 0.0018	0	0.0081	Estimated for the overall water depth in the basin (0.8 m); gas exchange was set to 0 when the roof was closed	This study

### 3 Discussion

#### 3.1 N<sub>2</sub>O concentrations in the SML

230 The overall average N<sub>2</sub>O enrichment factor indicated an enrichment of N<sub>2</sub>O in the SML. Please note, that the  
measurements of N<sub>2</sub>O in the SML are most probably underestimated because they were not corrected for the loss  
of N<sub>2</sub>O during sampling with the glass plate. A correction has been proven to be difficult because it depends on  
several, usually not quantified, factors and processes (see also Lange et al., 2025): 1) the dissolved gas saturation,  
because the exchange across the water/atmosphere interface on the glass plate is driven by the concentration  
235 difference between the atmosphere and the SML water. Thus, a high supersaturation will lead to an enhanced loss  
of gas compared to equilibrium saturations (and vice versa), 2) the amount of the surfactants in the SML. It is well-  
known that increasing amounts of surfactants can reduce the N<sub>2</sub>O exchange across the water/atmosphere interface  
(Mesarchaki et al., 2015), 3) the wind speed. When the glass plate is moved out of the water, the film of SLM  
water on the glass plate is exposed to enhanced wind speeds which can lead to an enhanced release of gas across  
240 the water/atmosphere interface, and 4) the physical properties of N<sub>2</sub>O, especially solubility and diffusivity, that  
are driven by temperature and salinity. Overall, there seems to be no constant loss factor and any estimate of the loss  
factor, e.g. in laboratory experiments, is thus challenging because it depends mainly on in-situ field conditions  
(e.g. the amount of the prevailing surfactants) which are difficult to mimic in laboratory experiments. Since no  
estimates of the N<sub>2</sub>O loss during glass plate sampling are available to our knowledge, the N<sub>2</sub>O concentrations in  
245 the SML presented here were not corrected. Based on the fact that we measured supersaturations of N<sub>2</sub>O in the  
SML despite the occurrence of surfactants in the SML (see Bibi et al., 2025), which counteract the N<sub>2</sub>O release to  
the atmosphere (Mesarchaki et al., 2015), we conclude that there must have been a significant enrichment of N<sub>2</sub>O  
in the SML during the course of the mesocosm study. This is in line with the suggestion of (Leon-Palmero et al.,  
2025) of a UV light-driven photochemical production of N<sub>2</sub>O (i.e. photochemodenitrification) which should be  
250 more enhanced in the SML because the SML is directly exposed to the sunlight.

#### 3.2 N<sub>2</sub>O saturations

N<sub>2</sub>O saturations in both the SML and the ULW were  $\geq 100\%$  during the course of the study. This supersaturation  
(= excess) of dissolved N<sub>2</sub>O was obviously resulting from a net in-situ production of N<sub>2</sub>O in the water. Therefore,  
the water in the mesocosm basin was a source for atmospheric N<sub>2</sub>O during the course of the study. The apparent  
255 increasing trend of the N<sub>2</sub>O saturations is resulting from the increasing temporal trends of the water temperature  
and the salinity (Fig. 1) which resulted in a reduced N<sub>2</sub>O solubility and therefore a decreasing trend in the N<sub>2</sub>O  
equilibrium concentrations while the measured N<sub>2</sub>O concentrations in the SML and the ULW showed no temporal  
trend (Fig. 3).

#### 3.3 Sources and sink of N<sub>2</sub>O

260 The accumulation of N<sub>2</sub>O concentrations in the SML and the ULW (as reflected by the persistent supersaturations  
in both layers, see section above) was resulting from its in-situ production. Potential N<sub>2</sub>O sources are  
photochemodenitrification, release from phytoplankton and microbial nitrification. The estimated photochemical  
production rates (PR<sub>pcd</sub>) from both the SML and the ULW (see Table 1) are at the lower end of the so far observed  
N<sub>2</sub>O production rates from photochemodenitrification in coastal and fresh water systems (Leon-Palmero et al.,  
265 2025). N<sub>2</sub>O production by marine phytoplankton can range from -0.06 to 0.99 nmol L<sup>-1</sup> h<sup>-1</sup> (McLeod et al., 2021).



The specific N<sub>2</sub>O production rate of *E. hux* (*G. hux*) as determined in a culture study was  $0.11 \pm 0.02$  nmol L<sup>-1</sup> h<sup>-1</sup> (McLeod et al., 2021). While there is no rate available for *C. closterium* culture study with other diatom species (incl. *Thalassiosira weissflogii*, *Thalassiosira pseudonana*, *Skeletonema marinoi* and *Cyclotella cryptica*) revealed N<sub>2</sub>O production rates from -0.01 to 0.3 nmol N<sub>2</sub>O L<sup>-1</sup> h<sup>-1</sup> (McLeod et al., 2021; Teuma et al., 2023) which are in the same range as the rates reported for *E. hux* (*G. hux*). N<sub>2</sub>O production rates via nitrification in oxic waters, such as found in the mesocosm study with dissolved oxygen concentrations >240 μmol L<sup>-1</sup> (Rauch et al., 2025) are usually low: For example, N<sub>2</sub>O production rates from ammonia oxidation (i.e. the first step of microbial nitrification) measured at the Bokins Eck coastal time-series site located in Eckernförde Bay (SW Baltic Sea) were found to range from 0.0001 to 0.0003 nmol N<sub>2</sub>O L<sup>-1</sup> h<sup>-1</sup> (Leon-Palmero et al., 2025). This is in line with the fact that prevailing high oxygen concentrations do not favour N<sub>2</sub>O production by nitrification (see e.g. Fig. 6 in Santoro et al., 2021). On the other hand, studies suggest that microenvironments around particles, including dead diatom aggregations, may provide oxygen depleted reaction space in which denitrification and N<sub>2</sub>O production may occur despite high dissolved oxygen concentrations within the surrounding water column (Ciccarese et al. 2023). However, the scale of N<sub>2</sub>O production around these particles is yet unknown. Therefore, the in-situ production of N<sub>2</sub>O during the mesocosm study was most likely resulting from photochemodenitrification and by the release from phytoplankton with only a minor contribution from nitrification.

The time-series of N<sub>2</sub>O concentrations in both the SML and ULW showed no temporal trends which indicate that the N<sub>2</sub>O concentrations were not affected by enhanced N<sub>2</sub>O production during the bloom, especially from the two bloom-dominating species *E. hux* (*G. hux*) and *C. closterium*. On the one hand, this seems to contrast the findings from various culture experiments which showed that haptophytes and diatoms have the potential to produce and release N<sub>2</sub>O (McLeod et al., 2021; Teuma et al., 2023). On the other hand, naturally as well as anthropogenically triggered phytoplankton blooms in the ocean did not result in enhanced N<sub>2</sub>O concentrations during the blooms (Farias et al., 2015; Law and Ling, 2001; Walter et al., 2005). The obvious negligible effect of the phytoplankton bloom on N<sub>2</sub>O concentrations during the mesocosm study (and other oceanic areas) does not exclude a N<sub>2</sub>O release from phytoplankton per-se, but suggests that N<sub>2</sub>O release was low and that the N<sub>2</sub>O production rates resulting from culture studies may not be representative for natural ecosystems.

The high-resolution 24h-sampling for N<sub>2</sub>O in the ULW took place during the pre-bloom phase (24 May 2023), during the bloom (2 June and 4 June 2023) and during the post-bloom phase (8 June 2023). Neither the different phases of the bloom nor the solar irradiation affected the N<sub>2</sub>O concentrations (Fig. 4). This finding, in combination with the missing trend over the entire period of the study, indicates that the N<sub>2</sub>O concentrations in both the SML and UWL were in a steady state where the in-situ sources were counterbalanced by the release of N<sub>2</sub>O to the overlying atmosphere: Rough estimates of the average N<sub>2</sub>O gas exchange in this study range from 0 to 6.5 nmol N<sub>2</sub>O L<sup>-1</sup> h<sup>-1</sup> (Table 1) and are, therefore, high enough to counteract the N<sub>2</sub>O production. Please note, however, that the approach of (Liss and Merlivat, 1986) does not account for the effect of surfactants. So, F<sub>ase</sub> is most probably overestimated. However, given the high uncertainties associated with the estimates of the sources and sink of N<sub>2</sub>O listed in Table 1, we can assume that the N<sub>2</sub>O sources were balanced by the N<sub>2</sub>O gas exchange flux. The photochemical production as well as the release by phytoplankton occurs during day time only because they are light-dependent. Because the roof of the mesocosm facility was closed during the night, the wind-driven N<sub>2</sub>O gas exchange took place only during day time as well. This might explain the absence of the diurnal cycles since both the sources and the sink of N<sub>2</sub>O were only active during the day but not during the night. This could have led to the establishment of a steady state during the day time which persisted during night time because sources and the

#### 4 Conclusions

N<sub>2</sub>O was measured during a mesocosm study in the ULW and, for the first time, in the SML. N<sub>2</sub>O concentrations were slightly enriched in the SML, although the difference of the mean N<sub>2</sub>O concentrations between the SML and  
310 ULW was statistically not significant. However, the enrichment of N<sub>2</sub>O in the SML was most probably underestimated due to the loss of N<sub>2</sub>O during sampling with the glass plate method. Consequently, a significant enrichment of N<sub>2</sub>O in the SML results in an enhanced N<sub>2</sub>O release to the atmosphere. Therefore, estimates of N<sub>2</sub>O emissions which do not account for the N<sub>2</sub>O enrichment in the SML most probably underestimate the N<sub>2</sub>O flux to the atmosphere. N<sub>2</sub>O was supersaturated in the SML and UWL during the course the mesocosm study which  
315 indicated an in-situ production of N<sub>2</sub>O. N<sub>2</sub>O in-situ production was most probably dominated by photochemodenitrification in combination with the release from phytoplankton. Microbial production of N<sub>2</sub>O via nitrification was assumed to be of minor importance because of the prevailing high oxygen concentrations which do not favour N<sub>2</sub>O production via nitrification. The N<sub>2</sub>O in-situ sources were obviously balanced by the release of N<sub>2</sub>O to the overlying atmosphere and thus the system was in a steady state. Therefore, N<sub>2</sub>O concentrations in both  
320 the SML and the UWL were remarkably constant over time showing no diurnal cycles and no enhanced N<sub>2</sub>O concentrations during the phytoplankton bloom. Our results are thus in line with the results from field studies which showed that phytoplankton blooms in the ocean do not result in temporarily enhanced N<sub>2</sub>O concentrations in the ocean surface layer.

The results presented here indicate that the role of the SML for N<sub>2</sub>O cycling in the surface ocean has been  
325 overlooked so far. It seems to be more important than previously thought. Future studies should, therefore, identify and quantify the N<sub>2</sub>O sources and sinks in the SML. Moreover, we plea to develop a sampling method which minimizes the loss of dissolved trace gases while sampling in order to get reliable N<sub>2</sub>O measurements from the SML to be used in estimates of the N<sub>2</sub>O emissions to the atmosphere.

#### Data availability

330 All data will be archived and made available to the scientific community via the PANGAEA database upon doi assignment. Data are available at any time from the authors upon request.

#### Author contribution

IS: conceptualization, formal analysis, investigation, supervision, visualisation, writing (original draft preparation), writing (review and editing). LL: conceptualization, formal analysis, investigation, writing (review  
335 and editing). HWB: conceptualization, formal analysis, funding acquisition, supervision, writing (review and editing).

#### Competing interests

HWB is a member of the editorial board of Biogeosciences.



### Acknowledgements

340 We would like to thank Hendrik Feil and all other colleagues of the BASS project for their role in the planning,  
set up and maintenance of the mesocosm study as well as during the sampling process. The authors would also  
like to thank the student assistants of our laboratory at GEOMAR Helmholtz Centre for Ocean Research Kiel,  
namely Isabell Hentschel, Laura Biet, Jonas Blendl, Romy Kreyenhagen, Daniel Brüggemann and Florian  
Schreiber, for their dedicated work in analysing the samples. We thank Oliver Wurl and Riaz Bibi for coordinating  
345 the mesocosm study.

### Financial support

This study was funded by the DFG Research Unit BASS (Biogeochemical processes and Air–sea exchange in the  
Sea-Surface microlayer) with grant no. 451574234.

### References

- 350 Asmussen-Schäfer, F., Ribas-Ribas, M., Wurl, O., and Friedrichs, G.: Linking surface coverage with surfactant  
activity to refine the role of surfactants for air–sea gas exchange, *EGUsphere*, 2025, 1–25, 2025.
- Bange, H. W., Mongwe, P., Shutler, J. D., Arévalo-Martínez, D. L., Bianchi, D., Lauvset, S. K., Liu, C., Löscher,  
C. R., Martins, H., Rosentreter, J. A., Schmale, O., Steinhoff, T., Upstill-Goddard, R. C., Wanninkhof, R., Wilson,  
S. T., and Xie, H.: Advances in understanding of air–sea exchange and cycling of greenhouse gases in the upper  
355 ocean, *Elementa: Sci. Anth.*, 12, 10.1525/elementa.2023.00044, 2024.
- Bibi, R., Ribas-Ribas, M., Jaeger, L., Lehnert, C., Gassen, L., Cortés, E., Wollschläger, J., Thölen, C., Waska, H.,  
Zöbelein, J., Brinkhoff, T., Athale, I., Röttgers, R., Novak, M., Engel, A., Barthelmeß, T., Karnatz, J., Reinthaler,  
T., Spriahailo, D., Friedrichs, G., Schäfer, F., and Wurl, O.: Biogeochemical dynamics of the sea-surface  
microlayer in a multidisciplinary mesocosm study, *EGUsphere*, 2025, 1–53, 2025.
- 360 Ciccacese, D., Tantawi, O., Zhang, I. H., Plata, D., and Babbin, A. R.: Microscale dynamics promote segregated  
denitrification in diatom aggregates sinking slowly in bulk oxygenated seawater, *Communications Earth &  
Environment*, 4, 275, 2023.
- Conrad, R. and Seiler, W.: Influence of the surface microlayer on the flux of nonconservative trace gases (CO, H<sub>2</sub>,  
CH<sub>4</sub>, N<sub>2</sub>O) across the ocean-atmosphere interface, *J. Atmos. Chem.*, 6, 83–94, 1988.
- 365 Cunliffe, M. and Wurl, O.: Guide to best practices to study the ocean’s surface. , Marine Biological Association  
of the United Kingdom, Plymouth, UK, 2014.
- Cunliffe, M., Engel, A., Frka, S., Gasparovic, B., Guitart, C., Murrell, J. C., Salter, M., Stolle, C., Upstill-Goddard,  
R., and Wurl, O.: Sea surface microlayers: A unified physicochemical and biological perspective of the air-ocean  
interface, *Progr. Oceanogr.*, 109, 104–116, 10.1016/j.pocean.2012.08.004, 2013.
- 370 Engel, A., Bange, H. W., Cunliffe, M., Burrows, S., Friedrichs, G., Galgani, L., Herrmann, H., Hertkorn, N.,  
Johnson, M., Liss, P. S., Quinn, P., Schartau, M., Soloviev, A., Stolle, C., van Pinxteren, M., Upstill-Goddard, R.,  
and Zäncker, B.: The ocean’s vital skin: Towards an integrated understanding of the ocean surface microlayer,  
*Front. Mar. Sci.*, 4, 10.3389/fmars.2017.00165, 2017.



- Fariás, L., Florez-Leiva, L., Besoain, V., Sarthou, G., and Fernández, C.: Dissolved greenhouse gases (nitrous oxide and methane) associated with the naturally iron-fertilized Kerguelen region (KEOPS 2 cruise) in the Southern Ocean, *Biogeosci.*, 12, 1925–1940, 10.5194/bg-12-1925-2015, 2015.
- IPCC, Masson-Delmotte, V., Zhai, P., Pirani, A., Connors, S. L., Péan, C., Berger, S., Caud, N., Chen, Y., Goldfarb, L., Gomis, M. I., Huang, M., Leitzell, K., Lonnoy, E., Matthews, J. B. R., Maycock, T. K., Waterfield, T., Yelekçi, O., Yu, R., and Zhou, B. (Eds.): *Climate Change 2021: The Physical Science Basis. Contribution of Working Group I to the Sixth Assessment Report of the Intergovernmental Panel on Climate Change*, Cambridge University Press, Cambridge, UK and New York, NY, USA, 2391 pp., 10.1017/9781009157896, 2021.
- Kock, A., Schafstall, J., Brandt, P., Dengler, M., and Bange, H. W.: Sea-to-air and diapycnal nitrous oxide fluxes in the eastern tropical North Atlantic Ocean, *Biogeosci.*, 9, 957–964, 2012.
- Lange, L., Booge, D., Feil, H., Karnatz, J., Stoltenberg, I., Bange, H. W., and Marandino, C. A.: Glass plate sampling efficiency for trace gases in the sea surface microlayer, *EGUsphere*, 2025, 1-30, 2025.
- Law, C. S. and Ling, R. D.: Nitrous oxide flux and response to increased iron availability in the Antarctic Circumpolar Current, *Deep-Sea Res. II*, 48, 2509–2527, 2001.
- Leon-Palmero, E., Morales-Baquero, R., Thamdrup, B., Löscher, C., and Reche, I.: Sunlight drives the abiotic formation of nitrous oxide in fresh and marine waters, *Science*, 387, 1198–1203, doi:10.1126/science.adq0302, 2025.
- Liss, P. S. and Merlivat, L.: Air-sea exchange rates: introduction and synthesis, in: *The Role of Air-Sea Exchange in Geochemical Cycling*, edited by: Buat-Ménard, P., Series C: Mathem. & Phys. Sciences, D. Reidel Publishing Company, Dordrecht, 113–127, 1986.
- McLeod, A. R., Brand, T., Campbell, C. N., Davidson, K., and Hatton, A. D.: Ultraviolet radiation drives emission of climate-relevant gases from marine phytoplankton, *J. Geophys. Res: Biogeosci.*, 126, e2021JG006345, 10.1029/2021JG006345, 2021.
- Mesarchaki, E., Kräuter, C., Krall, K. E., Bopp, M., Helleis, F., Williams, J., and Jähne, B.: Measuring air–sea gas-exchange velocities in a large-scale annular wind–wave tank, *Ocean Sci.*, 11, 121–138, 10.5194/os-11-121-2015, 2015.
- Plouviez, M., Shilton, A., Packer, M. A., and Guieysse, B.: Nitrous oxide emissions from microalgae: potential pathways and significance, *J. of Appl. Phycol.*, 31, 1–8, 10.1007/s10811-018-1531-1, 2019.
- Prinn, R. G., Weiss, R. F., Arduini, J., Arnold, T., DeWitt, H. L., Fraser, P. J., Ganesan, A. L., Gasore, J., Harth, C. M., Hermansen, O., Kim, J., Krummel, P. B., Li, S., Loh, Z. M., Lunder, C. R., Maione, M., Manning, A. J., Miller, B. R., Mitrevski, B., Mühle, J., O'Doherty, S., Park, S., Reimann, S., Rigby, M., Saito, T., Salameh, P. K., Schmidt, R., Simmonds, P. G., Steele, L. P., Vollmer, M. K., Wang, R. H., Yao, B., Yokouchi, Y., Young, D., and Zhou, L.: History of chemically and radiatively important atmospheric gases from the Advanced Global Atmospheric Gases Experiment (AGAGE), *Earth Syst. Sci. Data*, 10, 985–1018, 10.5194/essd-10-985-2018, 2018.
- Rauch, C., Deyle, L., Jaeger, L., Cortés-Espinoza, E. F., Ribas-Ribas, M., Karnatz, J., Engel, A., and Wurl, O.: Phytoplankton blooms affect microscale gradients of oxygen and temperature across the sea surface microlayer, *EGUsphere*, 2025, 1–32, 10.5194/egusphere-2025-4833, 2025.
- Rhee, T. S.: *The process of air-water gas exchange and its application*, PhD, Office of Graduate Studies, Texas A&M University, College Station, 272 pp., 2000.

- Santoro, A. E., Buchwald, C., Knapp, A. N., Berelson, W. M., Capone, D. G., and Casciotti, K. L.: Nitrification and nitrous oxide production in the offshore waters of the Eastern Tropical South Pacific, *Global Biogeochem. Cycles*, 35, e2020GB006716, 2021.
- 415 Siedler, G. and Peters, H.: Properties of sea water, in: *Oceanography*, edited by: Sündermann, J., Landolt-Börnstein, New Series, Springer Verlag, Berlin, 233–264, 1986.
- Teuma, L., Sanz-Luque, E., Guieysse, B., and Plouviez, M.: Are microalgae new players in nitrous oxide emissions from eutrophic aquatic environments?, *Phycology*, 3, 356–367, 2023.
- 420 Tian, H., Pan, N., Thompson, R. L., Canadell, J. G., Suntharalingam, P., Regnier, P., Davidson, E. A., Prather, M., Ciais, P., Muntean, M., Pan, S., Winiwarter, W., Zaehle, S., Zhou, F., Jackson, R. B., Bange, H. W., Berthet, S., Bian, Z., Bianchi, D., Bouwman, A. F., Buitenhuis, E. T., Dutton, G., Hu, M., Ito, A., Jain, A. K., Jeltsch-Thömmes, A., Joos, F., Kou-Giesbrecht, S., Krummel, P. B., Lan, X., Landolfi, A., Lauerwald, R., Li, Y., Lu, C., Maavara, T., Manizza, M., Millet, D. B., Mühle, J., Patra, P. K., Peters, G. P., Qin, X., Raymond, P., Resplandy, L., Rosentreter, J. A., Shi, H., Sun, Q., Tonina, D., Tubiello, F. N., van der Werf, G. R., Vuichard, N., Wang, J., Wells, K. C., Western, L. M., Wilson, C., Yang, J., Yao, Y., You, Y., and Zhu, Q.: Global nitrous oxide budget (1980–2020), *Earth Syst. Sci. Data*, 16, 2543–2604, 10.5194/essd-16-2543-2024, 2024.
- 425 Upstill-Goddard, R. C., Frost, T., Henry, G., Franklin, M., Murrell, J. C., and Owens, N. J. P.: Bacterioneuston control of air-water methane exchange determined with a laboratory gas exchange tank, *Global Biogeochem. Cycles*, 17, 1108, doi:1110.1029/2003GB002043, 2003.
- 430 Walter, S., Peeken, I., Lochte, K., Webb, A., and Bange, H. W.: Nitrous oxide measurements during EIFEX, the European Iron Fertilization Experiment in the subpolar South Atlantic Ocean, *Geophys. Res. Lett.*, 32, L 23613, doi:23610.21029/22005GL024619, 2005.
- Wanninkhof, R.: Relationship between wind speed and gas exchange over the ocean revisited, *Limnol. Oceanogr. Methods*, 12, 351–362, 10.4319/lom.2014.12.351, 2014.
- 435 Weiss, R. F. and Price, B. A.: Nitrous oxide solubility in water and seawater, *Mar. Chem.*, 8, 347–359, 1980.
- Wilson, S. T., Bange, H. W., Arévalo-Martínez, D. L., Barnes, J., Borges, A. V., Brown, I., Bullister, J. L., Burgos, M., Capelle, D. W., Casso, M., de la Paz, M., Fariás, L., Fenwick, L., Ferrón, S., Garcia, G., Glockzin, M., Karl, D. M., Kock, A., Laperriere, S., Law, C. S., Manning, C. C., Marriner, A., Myllykangas, J. P., Pohlman, J. W., Rees, A. P., Santoro, A. E., Tortell, P. D., Upstill-Goddard, R. C., Wisegarver, D. P., Zhang, G. L., and Rehder, G.: An intercomparison of oceanic methane and nitrous oxide measurements, *Biogeosci.*, 15, 5891–5907, 10.5194/bg-15-5891-2018, 2018.
- 440 Wurl, O., Ekau, W., Landing, W. M., and Zappa, C. J.: Sea surface microlayer in a changing ocean—A perspective, *Elementa: Sci. Anth.*, 5, 31, 2017.
- 445 Wurl, O., Ekau, W., Landing, W. M., and Zappa, C. J.: Corrigendum: Sea surface microlayer in a changing ocean – A perspective, with refocused context, *Elementa: Sci. Anth.*, 9, 10.1525/elementa.2021.00228.c, 2021.
- Wurl, O., Wurl, E., Johnson, K., and Vagle, S.: Formation and distribution of sea-surface microlayers, *Biogeosci.*, 8, 121–135, 2011.
- Zhou, L.-M., Sun, Y., Zhang, H.-H., and Yang, G.-P.: Distribution and characteristics of inorganic nutrients in the surface microlayer and subsurface water of the Bohai and Yellow Seas, *Cont. Shelf Res.*, 168, 1–10, 2018.
- 450